

www.acsanm.org Article

# Cellulose Nanocrystals Protect Plants from Pathogen Infection

Henry J. Squire, Minjae Kim, Cerise Wong, Amanda Seng, Autumn Y. Lee, Natalie S. Goh, Jeffery Wei-Ting Wang, and Markita P. Landry\*



Cite This: https://doi.org/10.1021/acsanm.3c06040

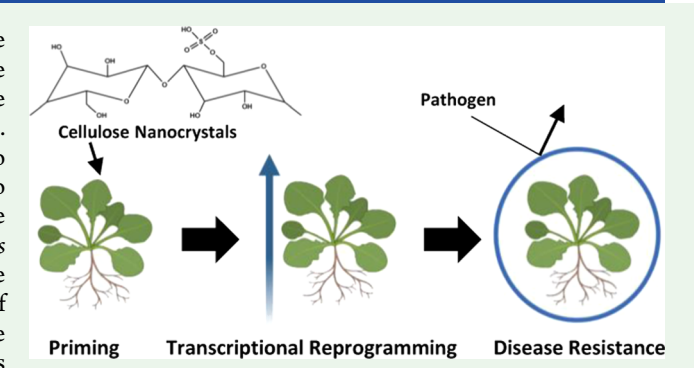


**ACCESS** 

III Metrics & More

Article Recommendations

ABSTRACT: Plants are capable of mounting an immune defense in response to infection, wounding, or environmental stress. The immune response of a plant is often mediated through the recognition of conserved molecular motifs associated with stress. Treating plants with these molecular motifs prior to exposure to stress, termed immune priming, can improve plant resilience to subsequent stressors. Here, we demonstrate the use of cellulose nanocrystals (CNCs) as an immune priming tool for *Arabidopsis thaliana* combining phenotypic and transcriptomic data to validate the efficacy of CNCs as an immune primer. Pretreatment of *Arabidopsis* with CNCs reduces the level of infection by the pathogen *Pseudomonas syringae* up to 65%. RNA sequencing shows that treatment of *Arabidopsis* with CNCs results in deep



transcriptional reprogramming, perturbing over 1300 genes, most of which are associated with immune regulation. We hypothesize plants recognize CNCs as cell-wall damage, potentially explaining the observed immune response. Finally, physiological characterization of the plant response to CNCs demonstrates minimal effects on plant growth without inducing callose deposition or generation of reactive oxygen species. This work provides a foundation for future investigation of cellulose-based nanomaterials as immune primers, particularly in crop species. Given their ease of synthesis, low cost, degradability, and bio/environmental compatibility, cellulose-based materials could serve as a complement to conventional biocides for pathogen control.

KEYWORDS: cellulose nanocrystals, plant immunity, systemic acquired resistance, immune priming, transcriptomics

## **■ INTRODUCTION**

Plants recognize molecular patterns associated with pathogen infection. Pathogen-associated molecular patterns (PAMPs), damage-associated molecular patterns (DAMPs), and pathogen effectors can all be recognized by plants as signals of infection. While plants are not thought to possess specialized immune cells, each individual cell in a plant is capable of recognizing infection and initiating an immune response. Recognition of PAMPs or DAMPs triggers resistance responses, which can include the production of reactive oxygen species, signaling hormones, and antimicrobial compounds as well as cell wall reorganization and transcriptional reprogramming. <sup>2,3</sup>

Resistance responses typically involve signaling between distal tissues, which enables plant-wide resistance even if infection is not initially widespread. This phenomenon is termed systemic acquired resistance (SAR). Infection is not a prerequisite for activation of plant immunity; chemical compounds or materials that mimic DAMPs/PAMPs can induce SAR and thus indirectly protect plants from pathogens. This process, termed immune priming, is a potential method for managing plant pathogens yet thus far does not have widespread adoption as immune priming tools typically have

negative impacts on plant growth and crop yield. Despite this, a wide variety of chemicals and materials are capable of immune priming and enhancing plant disease resistance. Chemicals such as benzothiadiazole and salicylic acid induce SAR and significantly enhance plant disease resistance but at the cost of plant growth. Similarly, peptides such as flg22 derived from bacteria that are pathogenic to plants enhance disease resistance also at the cost of plant growth. Polysaccharide-based materials, which potentially mimic cellwall damage, such as cellobiose and oligoglacturonides, can also enhance plant disease resistance.

Recently, nanomaterials such as silica nanoparticles<sup>9,10</sup> and chitosan nanoparticles<sup>11</sup> were also demonstrated to enhance plant resistance. Interestingly, immune priming via silica nanoparticles does not negatively impact plant growth, a

Received: December 20, 2023 Revised: February 15, 2024 Accepted: February 16, 2024



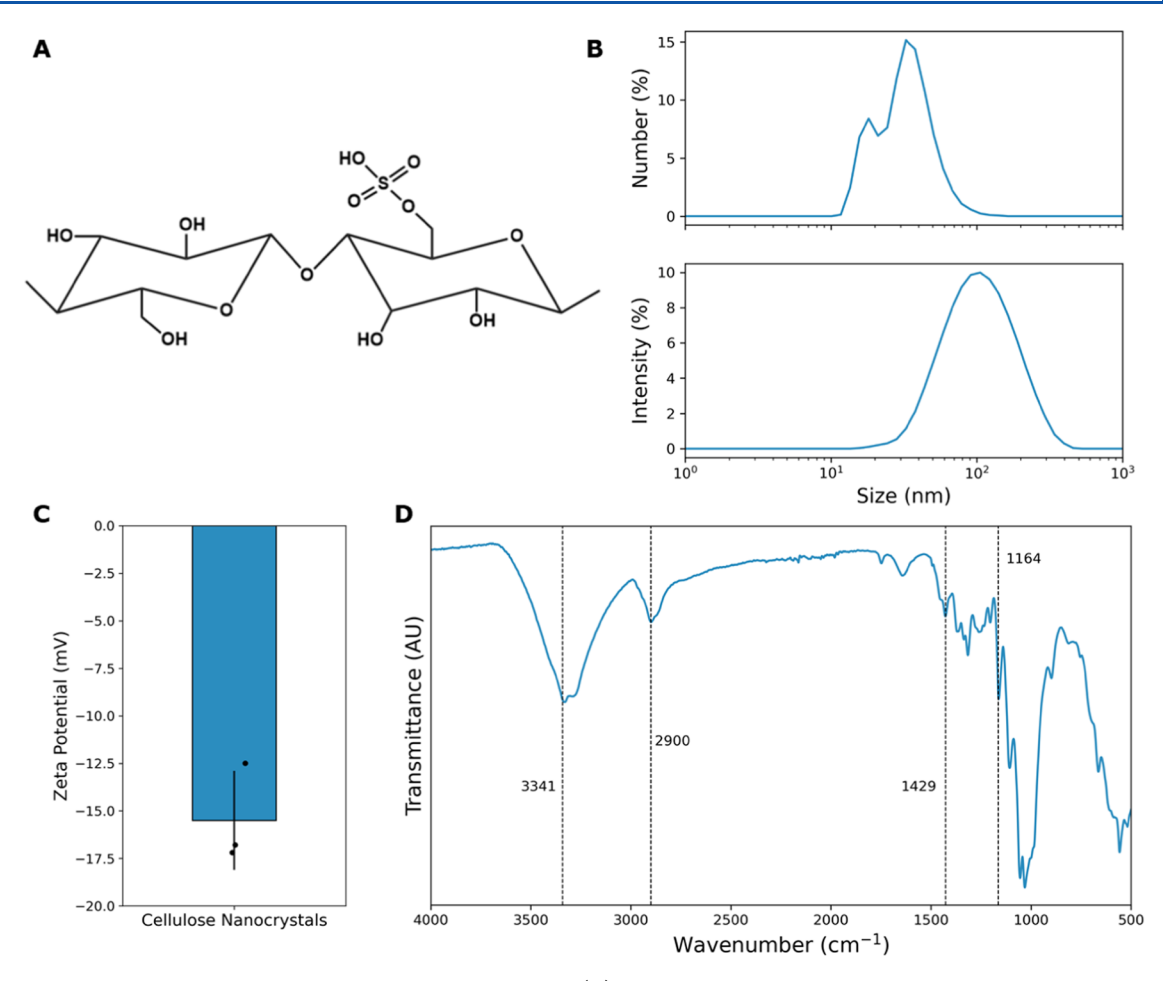


Figure 1. Physical characterization of the commercially procured CNCs. (A) Chemical structure of the CNC material with sulfate-half ester groups from the sulfuric acid hydrolysis synthesis process. (B) CNC size from dynamic light scattering experiments on a number (top) and intensity (bottom) basis. Mean size (number basis) was 34.1 nm, and mean size (intensity basis) was 157.6 nm. (C) ζ-potential measurements for CNCs suspended in water. Mean ζ-potential of -15.5 mV. Error bar represents the standard deviation of three replicate measurements. (D) ATR-FTIR spectra for CNC powder.

promising result that motivates further investigation of nanomaterial priming tools. 12 Outside plant disease resistance, nanomaterials have applications in plants as delivery tools for cargo such as nucleic acids, small molecules, proteins, fertilizers, and pesticides. As interest grows in utilizing nanomaterials in plant applications, understanding plantnanomaterial interactions is important to enable the rational design of nanotechnologies. Cellulose nanocrystals (CNCs) are a degradable, renewable nanomaterial with typical dimensions of 2-50 nm in diameter and 100-2000 nm in length. CNCs have drawn interest in a variety of fields due to their ease in synthesis and low cost; 13 in plant biotechnology applications, CNCs have reported uses in delivery of pesticides and frost protection of crops. 14,15 Given the growing interest in CNCs for plant biotechnology applications, here, we characterize the response of Arabidopsis thaliana to CNC exposure. We find CNCs enhance Arabidopsis resistance to the bacterium Pseudomonas syringae. The transcriptional response of the plant to CNC exposure, as evaluated by RNA sequencing, is consistent with the SAR activation. Physiological characterization of the plant response to CNCs suggests no negative effects on plant growth. This work informs future users of CNCs in plant applications and motivates additional investigation of the potential of protecting plants from disease with CNCs.

#### RESULTS AND DISCUSSION

CNCs were procured from CelluForce (produced via sulfuric acid hydrolysis). The chemical structure of the CNC material is shown in Figure 1A with sulfate-half ester groups. Material specifications from the supplier indicate an expected particle size of 150 nm (measured via dynamic light scattering) and a sulfur content of 5000-9000 mg/kg power. Independent characterization with dynamic light scattering confirms a mean particle size (intensity basis) of 157.6 nm (Figure 1B) with a  $\zeta$ potential of -15.5 mV (Figure 1C). We note CNCs are cylindrical with high aspect ratios; thus, dynamic light scattering is only an estimation of the average feature sizes. Accordingly, the size intensity profile is broad, and the size number profile displays multiple peaks. Further characterization with attenuated total reflectance (ATR)-Fourier transform infrared spectroscopy (FTIR) (Figure 1D) returned the expected CNC spectra with O-H stretching peak at 3341 cm<sup>-1</sup>, C-H stretching peak at 2900 cm<sup>-1</sup>, C-H bending peak at 1429 cm<sup>-1</sup>, and C-O-C glycosidic stretching peak at 1164 cm<sup>-1</sup>. <sup>16,17</sup> The CNCs were suspended in sterile water and used in plant-pathogen experiments without any modification.

Next, to evaluate CNCs as an immune priming tool, the model plant-pathogen system *A. thaliana* challenged with *P. syringae* was investigated. Leaves were syringe-infiltrated with

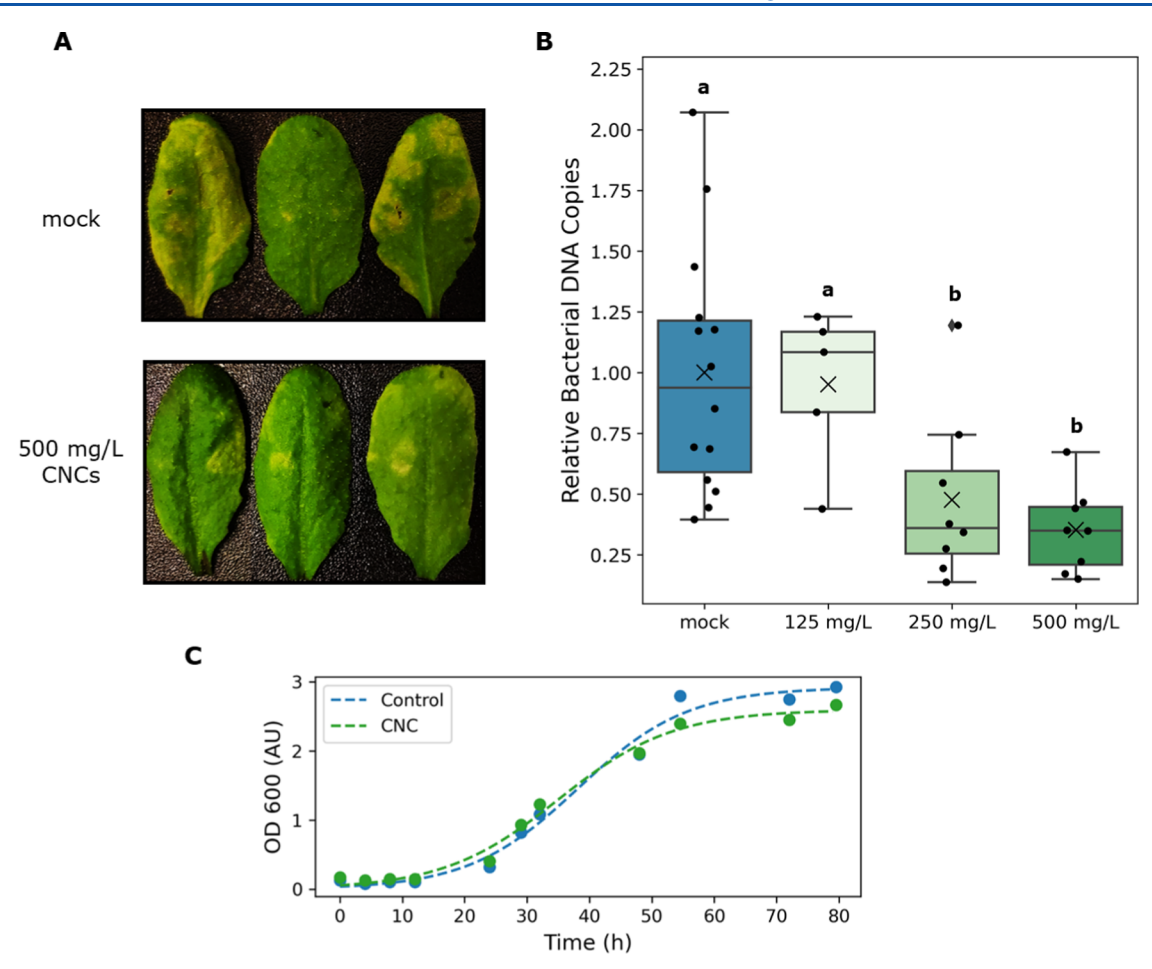


**Figure 2.** CNCs protect *A. thaliana* leaves from infection by *P. syringae*. (A) Representative leaves 3 dpi with *P. syringae*. Mock-treated and 500 mg/L CNC-treated leaves are displayed. (B) Extent of infection was quantified 3 dpi via qPCR. Relative Bacterial DNA Copies were determined by the ddCt method using the qPCR cycle count difference between the *A. thaliana* gene expG and the *P. syringae* gene oprF releative to a mock sample. Each point is taken from a pool of 3 leaves from an individual plant (N = 8). Statistical comparisons between each treatment were conducted with a Kruskal–Wallis test in combination with a Conover multiple comparison test. "X" marks the mean relative bacterial DNA copies. (C) Optical density of *P. syringae* liquid cultures grown over time in the absence (control) and presence of 500 mg/L CNCs (CNC).

three separate concentrations of CNCs, 500, 250, and 125 mg/ L, and challenged with P. syringae 24 h later. These concentrations (500, 250, and 125 mg/L) were chosen after observing negative plant health impacts at concentrations above 750 mg/L CNCs (data not shown). Previous work has demonstrated excessive doses of priming tools can increase plant susceptibility to infection by inducing stress responses; thus, it is not surprising excessive doses of CNCs can have negative impacts on plant health.9 For the dosage range studied here, up to 500 mg/L CNCs, negative plant health impacts were not observed. As compared to mock-treated plants, plants treated with 500 mg/L CNCs visually displayed fewer symptoms of infection, as shown in Figure 2A. Quantification of infection through PCR amplification of bacterial genomic DNA also suggested pretreatment of plants with 500 mg/L CNCs or with 250 mg/L CNCs reduced bacterial infection by 65 and 52% relative to mock-treated plants, respectively, Figure 2B. However, treatment at 125 mg/ L did not provide significant protection against P. syringae infection, suggesting CNCs enable pathogen protection in a dose-dependent manner. Previous cellulosic materials provided similar levels of protection; for example, oxidized cellulose oligosaccharides reduced infection of Arabidopsis by Botrytis cinerea by 60%. Next, to control for possible direct toxicity of

CNCs on *Pseudomonas*, bacterial cultures were grown in the presence and absence of 500 mg/L of CNCs. *Pseudomonas* growth was tracked by monitoring the optical density of the culture at 600 nm; no impact on *Pseudomonas* rate of growth or final population was observed, Figure 2C. This is in alignment with the current literature; previous investigations of CNC toxicity on bacteria found that viability was dependent on the concentration and surface chemistry of the CNCs as well as the species of bacteria. Results are variable, but for *Escherichia coli*, the dose of unfunctionalized CNCs, which negatively impacts bacterial growth, varies between 1200<sup>18</sup> and 17 000 mg/L, <sup>19</sup> 2.4–34 times greater than the concentrations used here. These data suggest CNCs immune prime *Arabidopsis* in a dose-dependent manner without directly affecting *Pseudomonas* viability.

To further characterize the response of *Arabidopsis* to CNC exposure, we performed a transcriptomic analysis of CNC-treated plants with RNA sequencing. Fourteen-day-old seedlings were mock treated or treated with 125 or 500 mg/L CNC; the transcriptional response was characterized 1 h after treatment. CNC treatment significantly perturbed seedling transcriptome; relative to the mock treatment, 1349 significantly differentially expressed genes (DEGs) were identified after treatment with 500 mg/L CNCs, as shown in Figure 3A.

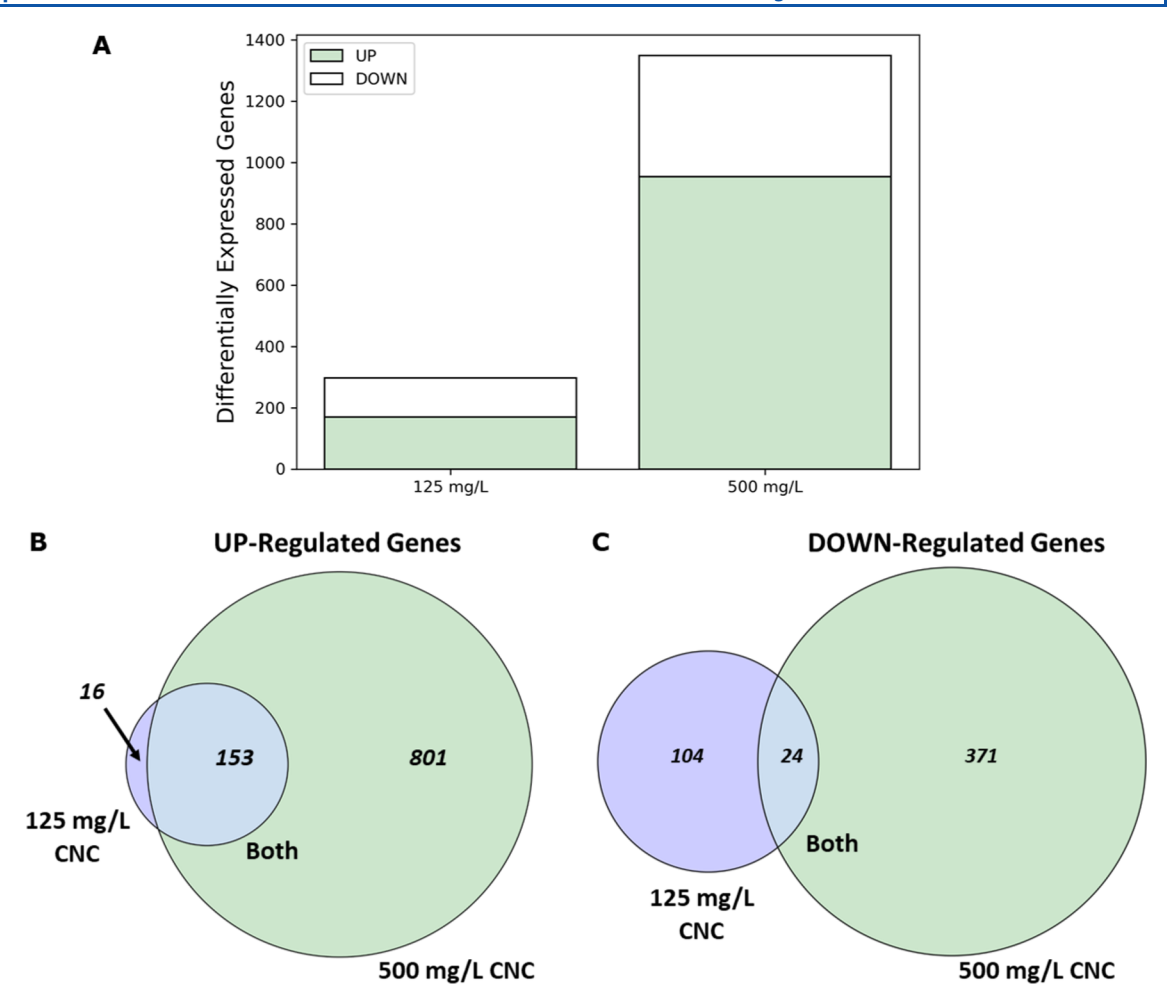


Figure 3. CNCs induce deep transcriptional reprogramming of Arabidopsis seedlings in a dose-dependent manner. (A) Number of significantly differentially expressed genes (relative to mock-treated plants) for each treatment (125 and 500 mg/L CNCs). Only genes with a false discovery rate < 0.05 are considered. Genes with  $\log_2(\text{fold change}) \leq -1$  are classified as downregulated while genes with  $\log_2(\text{fold change}) \geq 1$  are classified as upregulated. (B) Area weighted Venn diagram displaying statistically significant upregulated genes (relative to mock-treated plants) across 125 and 500 mg/L CNC or both treatments. (C) Area weighted Venn diagram displaying statistically significant downregulated genes (relative to mock-treated plants) across 125 and 500 mg/L CNC or both treatments.

In contrast, only 297 DEGs were identified after treatment with 125 mg/L CNCs, as shown in Figure 3A. Further investigation shows most DEGs that were upregulated in response to 125 mg/L CNC treatment are also upregulated in response to 500 mg/L CNC treatment, 153 DEGs, Figure 3B. However, in addition to these 153 DEGs, which were upregulated by both treatments, there are an additional 801 DEGs upregulated by treatment with 500 mg/L CNCs but not upregulated by treatment with 125 mg/L CNCs. Interestingly, repeating the same analysis with downregulated DEGs reveals less overlap between treatments, with only 24 DEGs downregulated by both treatments, Figure 3C. Despite the lack of overlap, treatment with 500 mg/L CNCs still results in a greater number of unique downregulated DEGs (371) as compared to treatment with 125 mg/L CNCs (104). Taken together, the RNA sequencing results are in alignment with the results of the pathogen protection assay; Arabidopsis responds to CNCs in a dose-dependent manner.

Compared to the 500 mg/L CNC treatment, previous transcriptomic profiling of other cellulosic-based immune elicitors identified fewer DEGs. For example, 1 h after treatment of *Arabidopsis* seedlings with oxidized cellulose oligosaccharides, a total of 545 DEGs were identified.<sup>8</sup>

Similarly, for cellobiose, 689 DEGs were found, though at earlier time points than what was investigated here.<sup>20</sup> However, other noncellulosic elicitors such as oligogalacturonides (a DAMP derived from pectin) and flg22 (a well-characterized peptide PAMP) induced more transcriptomic changes than CNCs with 1672 DEGs and 4413 DEGs reported, respectively.<sup>21</sup> Furthermore, as with our observed results with CNCs, oligogalacturonides were observed to induce transcriptional changes in a dose-dependent manner.<sup>21</sup> In general, flg22 is among the strongest elicitors of immunity known in Arabidopsis, providing significant pathogen protection, stunting plant growth, and inducing deep transcriptional reprogramming.<sup>7,21</sup> Treatment with 500 mg/L CNCs induces a response that is stronger than previously reported cellulosic materials but weaker than flg22. For practical application, the weaker eliciting of CNCs as compared to flg22 could be advantageous from the perspective of growth immunity trade-

Next, gene ontology (GO) was leveraged to relate DEGs to biological processes. Specifically, upregulated DEGs from the 125 and 500 mg/L CNC treatments were investigated further. The GO terms associated with DEGs upregulated by 500 mg/L CNC treatment were mostly associated with immune

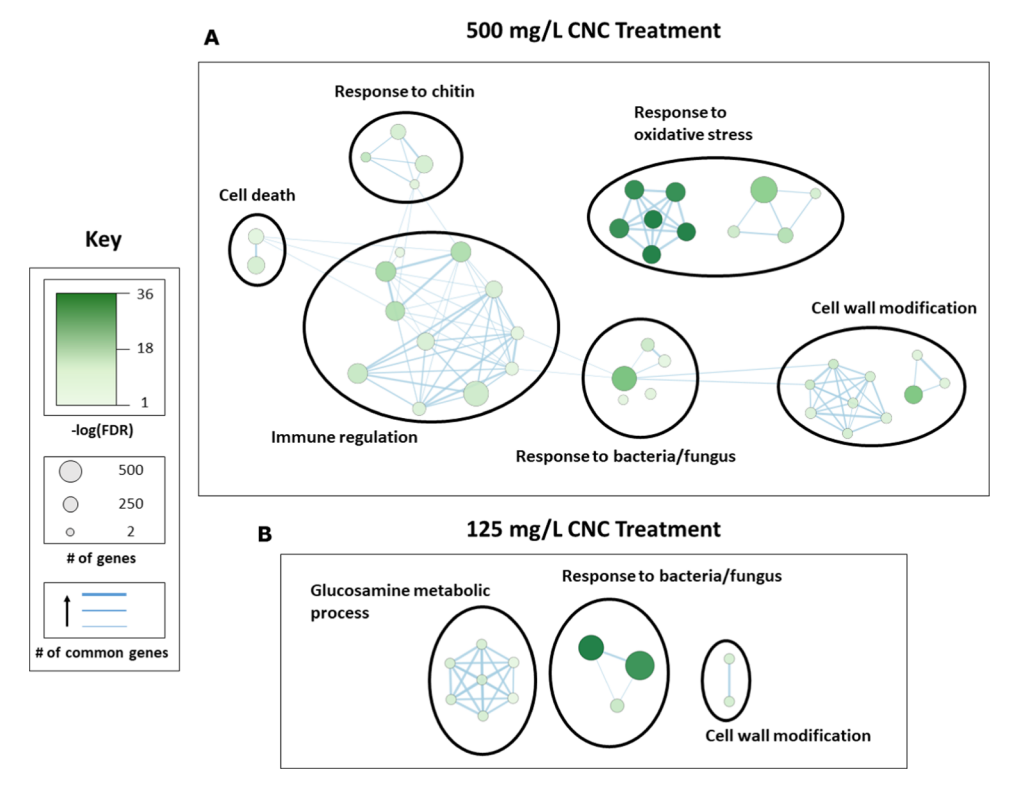


Figure 4. CNC treatment results in differential regulation of genes associated with immune defense. (A) Partial gene ontology network of statistically significantly upregulated genes from treatment with 500 mg/L CNCs. (B) Gene ontology network of statistically significantly upregulated genes from treatment with 125 mg/L CNCs.

processes and responses to stress, Figure 4A. Clustering similar GO terms reveals that biological processes such as immune regulation, response to bacteria, and response to oxidative stress are perturbed by treatment with 500 mg/L CNCs. A cluster of DEGs associated with cell wall modification is also observed; given CNCs are derived from cellulose, the primary biopolymer comprising the plant cell wall, it is possible cells interpret CNCs as cell wall damage. Broadly, these results for the 500 mg/L CNC treatment are in alignment with previous transcriptomic studies of plant response to other cellulosic materials. 8,20 Oxidized cellulose oligosaccharides and cellobiose are both reported to perturb gene clusters associated with immune regulation and response to bacteria.8 Furthermore, as with the 500 mg/L CNC treatment, both oxidized cellulose oligosaccharides and cellobiose perturb genes associated with cell wall organization. Previous work suggested cellulose oligosaccharides and cellobiose are recognized as DAMPs by plasma membrane-anchored receptor proteins.8 We hypothesize CNCs are recognized similarly, although future work must confirm this hypothesis with knockout lines.

Repeating the analysis with DEGs upregulated due to treatment with 125 mg/L CNCs identifies fewer GO clusters, Figure 4B. The identified clusters are associated with immune processes but with weaker statistical significance and fewer total DEGs. In summary, GO suggests treatment with 500 mg/L CNCs induces immune priming in *Arabidopsis* plants, which may explain subsequent resistance to infection. In contrast, treatment with 125 mg/L CNC does not significantly perturb the immune state of the plant and thus does not immune prime or enable disease resistance. GO analysis provides further evidence that CNC immune priming occurs in a dose-dependent manner.

As a complement to the transcriptomic analysis, the physiological response of the Arabidopsis tissue to CNC treatment was characterized. First, production of reactive oxygen species (ROS) is characterized. Exposure to immune elicitors typically results in a burst of metabolic activity visible as production of ROS. We therefore sought to identify whether CNC treatment of Arabidopsis generated an ROS burst. To do so, we compared treatment with 500 mg/L CNCs to flg22 treatment, a positive control for ROS burst. Interestingly, treatment with 500 mg/L CNCs does not induce a ROS burst, in contrast to flg22, as characterized through a luminol assay, Figure 5A. These results are in alignment with previous work investigating other cellulosic-based materials, which also do not induce ROS.8 Next, the plant growth response to CNCs was characterized. The trade-off between growth and immunity is well documented; typically, immune elicitors hamper plant growth and crop yields.5 To evaluate the impact of CNCs on Arabidopsis growth, seedlings were grown for 10 days, treated with CNCs on day 10, and grown for an additional 7 days. Notably, treatment with 125 or 500 mg/L CNCs reduced growth by 7 and 11%, respectively, relative to mock-treated plants, Figure 5B. As a positive control, seedlings were also grown in the presence of flg22. In this case, plant growth was stunted with plants obtaining 53% less mass. Thus, similar to silica nanoparticles, CNCs minimally interfere with plant growth. This is an encouraging result suggesting CNCs could safely serve roles in plant biotech applications without negative impacts on crop yield. Finally, we note that several GO terms associated with genes upregulated by 500 mg/L CNC treatment, aside from stress, were associated with plant cell wall modifications and damage. Therefore, we sought to characterize whether CNC plant treatment induced cell wall modification. Upon exposure to PAMPs or DAMPs, plant cells

ACS Applied Nano Materials www.acsanm.org

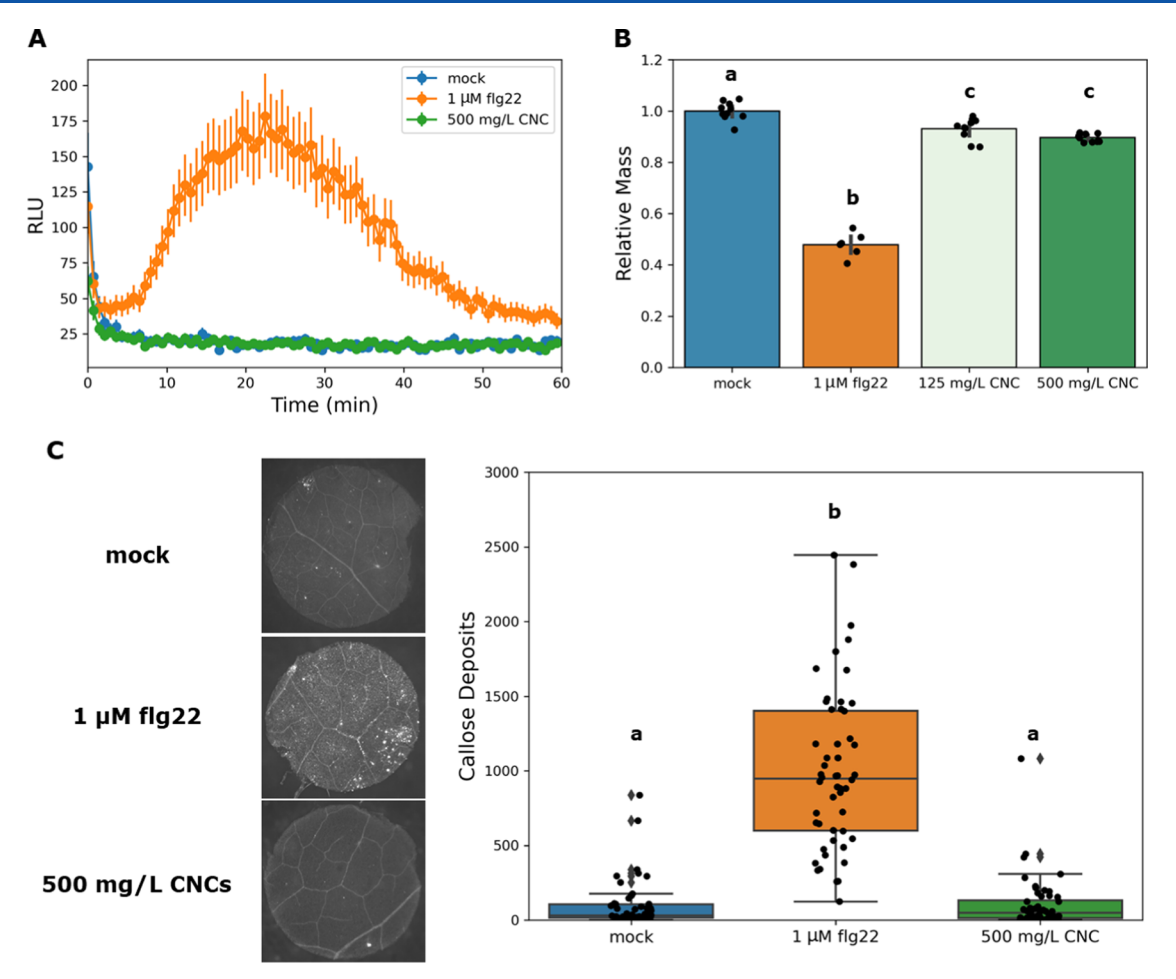


Figure 5. Physiological characterization of Arabidopsis response to CNC treatment. (A) is a luminol-based assay characterizing production of ROS after mock, flg22, or CNC treatment. Each treatment was tested with 6 separate leaf discs taken from 5-week-old Arabidopsis (N = 3). (B) Arabidopsis seedling mass after growth under various treatments normalized to the mock condition. Each point is the normalized mass of a group of 10 seedlings (N = 3). Statistical comparisons between each treatment were conducted with a Kruskal—Wallis test in combination with a Conover multiple comparison test with a Bonferroni correction. (C) 5-week-old Arabidopsis characterized for callose after treatment under various conditions. Left, representative field of views. Bright spots are callose puncta stained with aniline blue. Right, quantification of the number of callose puncta per area of the leaf disc imaged. A point represents a single leaf disc, and a total of 8 distinct plants were screened per treatment (N = 8). Statistical comparisons between each treatment were conducted with a Kruskal—Wallis test in combination with a Conover multiple comparison test with a Bonferroni correction.

commonly reinforce their cell wall with callose to protect from pathogens. To evaluate callose deposition, leaves of 5-week-old Arabidopsis were treated with 500 mg/L CNCs or 1  $\mu$ M flg22 as a positive control and stained for callose with aniline blue. Compared to flg22, treatment with CNCs did not induce significant callose deposition, as shown in Figure 5C. Previous work has found certain cellulosic materials induce callose deposition. However, cellobiose, the minimal repeat component of cellulose, does not induce callose deposition. Thus, our findings are in alignment with previous reports.

#### CONCLUSIONS

Globally, plant pathogens reduce major crop yields by 20–30% and cause US\$220 billion in economic damage annually.<sup>23</sup> Current plant-pathogen management strategies rely primarily on the use of biocides, which can place extreme selective pressures on pathogens, driving evolution of resistant strains.<sup>24</sup> While biocides will likely remain a primary pathogen control strategy, as the sustainability of agricultural practices in general is re-evaluated, alternative pathogen control strategies such as induced SAR could play a role in protecting crops, especially in

the context of integrated pest/pathogen management strategies. Here, we characterized the pathogen-protective effect of cellulose nanocrystals on A. thaliana. Interestingly, we found that CNCs elicit an immune response in Arabidopsis, which confers disease resistance to P. syringae. Exposure to CNCs elicits deep transcriptional reprogramming in Arabidopsis, perturbing over 1300 genes after treatment with 500 mg/L CNCs. Many of the differentially regulated genes are involved in plant immunity, perhaps explaining the observed disease resistance. Specifically, gene clusters disturbed by the 500 mg/ L CNC treatment are involved in immune regulation, oxidative stress, and cell wall modification. Furthermore, given CNCs are derived from cell wall material, we hypothesize CNCs serve as a DAMP, mimicking cell wall damage, thus initiating the observed immune responses. This is supported by previous work on plant response to cellulosic materials, which suggested DAMP protein receptors recognized a variety of cellulosic materials and initiated downstream immune responses upon recognition. A variety of materials derived from different components of the cell wall have recently been reported as capable of eliciting disease resistance in plants. Historically,

Article

materials for induced SAR have not played a major practical role in protection of crops from pathogens, primarily due to growth immunity trade-offs. <sup>5</sup> Of note, CNCs do not appear to suffer from this trade-off.

This Letter provides preliminary evidence that CNCs could play a role as a tool to induce SAR in plants and highlights possible unanticipated immunological effects of utilizing CNCs in delivery applications for agriculture. To fully evaluate the utility of CNCs as a pathogen management tool, additional work is needed. First, in this study, CNCs were introduced to the plant via syringe infiltration; other application methodologies should be explored including atomization or spraying. Furthermore, while we hypothesize that Arabidopsis recognizes CNCs as cell wall damage, additional work in knockout lines is needed to rigorously evaluate the mechanism by which CNCs are recognized and induce immunity. Next, while we evaluated the protective effect of CNCs in Arabidopsis, additional work is needed in nonmodel species to evaluate if CNCs provide protection across plant species, particularly in crops. Finally, while we characterized protection from a model bacterial plant pathogen, P. syringae, future work should evaluate the breadth of pathogen species which CNCs can provide protection against.

# MATERIALS AND METHODS

**Materials.** CNCs were purchased from CelluForce. The material was produced via sulfuric acid hydrolysis and spray dried. The CNCs were used as received, suspended in sterile water at a particular treatment concentration (i.e., 500, 250, or 125 mg/L).

**Characterization.** The size distribution of the commercially procured CNCs was evaluated with dynamic light scattering with a Malvern Zetasizer Nano. CNCs at a concentration of 25 mg/L in deionized were analyzed three separate times at 25 °C. Similarly, the  $\zeta$ -potential of the CNCs was measured with a Malvern Zetasizer Nano at a concentration of 25 mg/L, three separate times at 25 °C. Attenuated total reflectance FTIR spectroscopy was conducted with a Bruker Vertex 80 V Spectrometer on CNC powder. A total of 64 scans from wavenumber 4000–400 cm<sup>-1</sup> with a resolution of 2 cm<sup>-1</sup> were taken.

**Plant Growth Conditions.** Mature A. thaliana (Col-0) was grown in growth chambers at 22 °C under 8 h days with a light flux of 100  $\mu$ mol m<sup>-2</sup> s<sup>-1</sup>. Seeds were sown on Sunshine Mix #4 soil in square 2.5 inch pots with ~3 seeds per pot. Pots were stratified in the dark at 4 °C for 3 days prior to germination. After stratification, seeds were germinated with humidity domes for 2 weeks. Seedlings were culled to a single plant per pot after 2 weeks, the humidity dome removed and left to grow for an additional 3 weeks for a total of 5 weeks. Plants were fertilized every other week with 20–20–20 fertilizer at a concentration of 150 ppm of total nitrogen. Plants were bottom watered weekly.

A. thaliana (Col-0) seedlings were grown in a growth chamber at 22 °C under 8 h days under a light flux of  $100~\mu \text{mol m}^{-2}~\text{s}^{-1}$ . Prior to sowing, seeds were sterilized by a brief 30 s incubation in 80% ethanol followed by a 15 min incubation in 50-50~(v/v) water-bleach solution and  $5\times$  rinses with sterile water. Seeds were then sown in 12-well plates supplemented with 1 mL of growth medium (half-strength Murashige and Skoog medium with 1% sucrose (w/v)) at a density of 10 seeds per well. Plates were stratified in the dark for 3 days at 4 °C and then transferred to germinate in growth chambers for 2 weeks.

Pathogen Challenge. Mature (5 week old) A. thaliana was used for pathogen challenge assays. Leaves number 10, 11, and 12 on the rosette (cotyledons serving as leaves 1 and 2) were gently infiltrated with treatments (125 or 500 mg/L CNCs suspended in sterile water) on the abaxial side using 1 mL syringes. Mock plants were infiltrated with sterile water. After treatment, the plants were returned to the growth chamber. Next, 24 h after treatment, plants were challenged with P. syringae pv tomato (DC3000). Prior to use, the culture was

recovered from a glycerol stock on King's Medium agar plates at 30  $^{\circ}\mathrm{C}$  for 2 days. Culture was scraped from the plate, suspended in 10 mM MgCl<sub>2</sub>, and diluted to an OD<sub>600</sub> of 0.002. Leaves, which were treated the previous day, were then gently syringe-infiltrated with dilute culture from the abaxial side. Excess culture was gently removed from leaves, and plants were returned to growth chambers with humidity domes. Finally, 3 days post pathogen challenge, infiltrated leaves from each plant were collected, pooled, and flash frozen in liquid nitrogen. In total, experiments consisted of 4 plants per treatment condition (3 pooled leaves per plant) repeated two independent times for a total of 8 plants per treatment condition (3 pooled leaves per plant).

To quantify the infection, genomic DNA was extracted from each pool of leaves via the cTAB method. Briefly, frozen leaves were grinded to powder and lysed with 700  $\mu \rm L$  of cTAB (2% w/v) at 65 °C for 45 min. Insoluble material was pelleted by centrifuging, the supernatant separated and then treated with RNase (0.1 mg/mL) at 37 °C for 20 min. Next, 700  $\mu \rm L$  of chloroform/isopropanol (39:1) was added. Samples were vortexed, followed by centrifuging. The upper aqueous layer was separated and treated with 700  $\mu \rm L$  of ice cold isopropyl alcohol to precipitate gDNA. Samples were centrifuged again to pellet gDNA. After decanting isopropyl alcohol, the pellet was washed with 70% ethanol, briefly dried, and resuspended in water.

Extracted gDNA was then used as a template for qPCR. Primers specific to the *P. syringae* gene oprF and primers specific to the *A. thaliana* gene expG (sequences in Table 1) were used to quantify

Table 1. Primers Used in This Study

primer	sequence $(5'-3')$
expG FWD	GAGCTGAAGTGGCTTCCATGAC
expG REV	GGTCCGACATACCCATGATCC
oprF FWD	AACTGAAAAACACCTTGGGC
oprF REV	CCTGGGTTGTTGAAGTGGTA

infection. Reactions were setup with 50 ng of gDNA, 0.5  $\mu$ M of forward primer, 0.5  $\mu$ M of reverse primer, and 1× PowerUp SYBR Green Master Mix for a total of 10  $\mu$ L. Reactions were run in triplicate on a BioRad CXF96 instrument. Raw cycle count outputs were analyzed via the ddCt method, where relative bacterial DNA copies is equal to the ratio of the difference between the expG gene (*A. thaliana*) counts and the oprF gene (*P. syringae*) counts for a treatment condition and mock sample. <sup>25</sup>

**Pathogen Growth Inhibition.** To evaluate if *P. syringae* growth is inhibited by CNCs, liquid cultures at a starting  $OD_{600}$  of 0.1 were supplemented with CNC and compared to an unsupplemented culture. Cultures were grown for 80 h at 30 °C in King's B media. The  $OD_{600}$  of the cultures was checked periodically over this time period.

RNA Sequencing. For RNA sequencing experiments, 14-day-old Arabidopsis seedlings were used. Seedlings were treated with liquid media supplemented with 125 or 500 mg/L CNCs. Mock-treated seedlings were treated with liquid media. One hour post treatment, seedlings were collected into 12 pools (4 pools per treatment group, 10 seedlings per pool). Pools were flash frozen, and total RNA was extracted using RNeasy Plant Mini Kit (Qiagen) per the manufacturer's protocol. RNA was library-prepped for sequencing using the NEBNext Ultra RNA Library Prep Kit for Illumina (New England Biolabs).

Reads were STAR aligned to the TAIR 10.1 reference genome. DESeq2 was used to conduct the differential expression analysis. After alignment, data were filtered such that only genes with a  $\log_2$  fold change less than -1 or greater than 1 with a false discovery rate statistic less than 5% were considered in downstream analysis. Gene ontology analysis was conducted with g:Profiler and visualized with Cytoscape.

**Oxidative Burst.** Oxidative burst induced via elicitors was evaluated via a luminol assay. Discs were cut from mature 5-week-old *Arabidopsis* leaves and carefully floated on 200  $\mu$ L of water DI overnight in a 96 well plate. The following day, water was replaced

with 200  $\mu$ L of solution containing 30  $\mu$ g/mL luminol and 20  $\mu$ g/mL horseradish peroxidase. Treatments were then added to the appropriate wells (mock, 1  $\mu$ M flg22, and 500 mg/L CNCs). Luminescence of each well was then tracked with a Tecan infinite M1000 Pro. Luminescence measurements were collected every 40 s for 1 h with an integration time of 1000 ms.

**Growth Inhibition.** To evaluate the impact of CNCs on plant growth, 10-day-old *Arabidopsis* seedlings grown in 12-well culture plates were challenged. On the tenth day of growth, liquid media was replaced with 1 mL of fresh liquid media, fresh liquid media supplemented with CNCs, or liquid media supplemented with flg22. Seedlings were grown for an additional 7 days and then collected, pooled, and weighed. Each pool consisted of 10 seedlings taken from a single well, and 3 pools per treatment group were considered for a single plate. Three distinct plates (biological replicates) were analyzed.

**Callose Assay.** Callose deposition was screened in mature (5 week old) *A. thaliana*. Leaves 10 and 11 were abaxially syringe-infiltrated with water (mock), 500 mg/L CNC, or 1  $\mu$ M of flg22. One day post infiltration, leaves were hole-punched away from the site of infiltration and cleared overnight in a solution of 1:3 v/v acetic acid/ethanol. After clearing, leaves were rinsed with 100 mM K<sub>2</sub>PO<sub>4</sub> for 1 h and then stained in analine blue for 2 h before a final rinse with 100 mM K<sub>2</sub>PO<sub>4</sub>. Discs were then imaged on a Zeiss AxioZoom V16 instrument with a DAPI filter. Callose deposits were quantified with a custom MATLAB script.

# AUTHOR INFORMATION

## **Corresponding Author**

Markita P. Landry — Department of Chemical and Biomolecular Engineering, University of California, Berkeley, Berkeley, California 94720, United States; Chan Zuckerberg Biohub, San Francisco, California 94158, United States; California Institute for Quantitative Biosciences, University of California, Berkeley, Berkeley, California 94720, United States; Innovative Genomics Institute, Berkeley, California 94720, United States; orcid.org/0000-0002-5832-8522; Email: landry@berkeley.edu

# Authors

- Henry J. Squire Department of Chemical and Biomolecular Engineering, University of California, Berkeley, Berkeley, California 94720, United States; orcid.org/0000-0002-7125-6885
- Minjae Kim Department of Chemical and Biomolecular Engineering, University of California, Berkeley, Berkeley, California 94720, United States
- Cerise Wong Department of Chemical and Biomolecular Engineering, University of California, Berkeley, Berkeley, California 94720, United States
- Amanda Seng Chan Zuckerberg Biohub, San Francisco, California 94158, United States
- Autumn Y. Lee Department of Chemistry, Amherst College, Amherst, Massachusetts 01002, United States; ⊚ orcid.org/ 0009-0004-1860-5187
- Natalie S. Goh Department of Chemical and Biomolecular Engineering, University of California, Berkeley, Berkeley, California 94720, United States
- Jeffery Wei-Ting Wang Department of Chemical and Biomolecular Engineering, University of California, Berkeley, Berkeley, California 94720, United States

Complete contact information is available at: https://pubs.acs.org/10.1021/acsanm.3c06040

#### Notes

The authors declare no competing financial interest.

# ACKNOWLEDGMENTS

Imaging experiments were conducted at the CNR Biological Imaging Facility at the University of California, Berkeley. RNA Sequencing experiments were conducted with support from the Chan Zuckerberg Biohub. The authors would like to thank Ruby Nelson and Christo Acosta for maintaining plants for experiments. H.J.S. is supported by the DoD through the NDSEG graduate fellowship. N.S.G. is supported by a FFAR Fellowship. J.W.W. is supported by the NSF through the GFRP. The authors further acknowledge support of a Burroughs Wellcome Fund Career Award at the Scientific Interface (CASI) (to M.P.L.), a Dreyfus foundation award (to M.P.L.), the Philomathia foundation (to M.P.L.), an NIH MIRA award (to M.P.L.), an NIH R03 award (to M.P.L.), an NSF CAREER award (to M.P.L.), an NSF CBET award (to M.P.L.), an NSF CGEM award (to M.P.L.), a CZI imaging award (to M.P.L.), a Sloan Foundation Award (to M.P.L.), a USDA BBT EAGER award (to M.P.L.), a Moore Foundation Award (to M.P.L.), an NSF CAREER Award (to M.P.L.), a Schmidt Foundation Polymaths Award (to M.P.L.), and a DOE Office of Science grant with award number DE-SC0020366 (to M.P.L.). M.P.L. is a Chan Zuckerberg Biohub investigator, a Hellen Wills Neuroscience Institute Investigator, and an IGI Investigator.

# REFERENCES

- (1) Zhou, J.-M.; Zhang, Y. Plant Immunity: Danger Perception and Signaling. *Cell* **2020**, *181* (5), 978–989.
- (2) Tang, D.; Wang, G.; Zhou, J.-M. Receptor Kinases in Plant-Pathogen Interactions: More Than Pattern Recognition. *Plant Cell* **2017**, 29 (4), 618–637.
- (3) Falak, N.; Imran, Q. M.; Hussain, A.; Yun, B.-W. Transcription Factors as the "Blitzkrieg" of Plant Defense: A Pragmatic View of Nitric Oxide's Role in Gene Regulation. *Int. J. Mol. Sci.* **2021**, 22 (2), 522 DOI: 10.3390/ijms22020522.
- (4) Gao, Q.-M.; Zhu, S.; Kachroo, P.; Kachroo, A. Signal Regulators of Systemic Acquired Resistance. *Front. Plant Sci.* **2015**, *06*, 228 DOI: 10.3389/fpls.2015.00228.
- (5) Yassin, M.; Ton, J.; Rolfe, S. A.; Valentine, T. A.; Cromey, M.; Holden, N.; Newton, A. C. The Rise, Fall and Resurrection of Chemical-induced Resistance Agents. *Pest Manage. Sci.* **2021**, *77* (9), 3900–3909.
- (6) Buswell, W.; Schwarzenbacher, R. E.; Luna, E.; Sellwood, M.; Chen, B.; Flors, V.; Pétriacq, P.; Ton, J. Chemical Priming of Immunity without Costs to Plant Growth. *New Phytol.* **2018**, 218 (3), 1205–1216.
- (7) Felix, G.; Duran, J. D.; Volko, S.; Boller, T. Plants Have a Sensitive Perception System for the Most Conserved Domain of Bacterial Flagellin: Plants Perceive a Conserved Domain of Bacterial Flagellin. *Plant J.* **1999**, *18* (3), 265–276.
- (8) Zarattini, M.; Corso, M.; Kadowaki, M. A.; Monclaro, A.; Magri, S.; Milanese, I.; Jolivet, S.; de Godoy, M. O.; Hermans, C.; Fagard, M.; Cannella, D. LPMO-Oxidized Cellulose Oligosaccharides Evoke Immunity in Arabidopsis Conferring Resistance towards Necrotrophic Fungus B. Cinerea. Commun. Biol. 2021, 4 (1), 727.
- (9) El-Shetehy, M.; Moradi, A.; Maceroni, M.; Reinhardt, D.; Petri-Fink, A.; Rothen-Rutishauser, B.; Mauch, F.; Schwab, F. Silica Nanoparticles Enhance Disease Resistance in Arabidopsis Plants. *Nat. Nanotechnol.* **2021**, *16* (3), 344–353.
- (10) Du, J.; Liu, B.; Zhao, T.; Xu, X.; Lin, H.; Ji, Y.; Li, Y.; Li, Z.; Lu, C.; Li, P.; Zhao, H.; Li, Y.; Yin, Z.; Ding, X. Silica Nanoparticles Protect Rice against Biotic and Abiotic Stresses. *J. Nanobiotechnol.* **2022**, *20* (1), 197.

- (11) Chandra, S.; Chakraborty, N.; Dasgupta, A.; Sarkar, J.; Panda, K.; Acharya, K. Chitosan Nanoparticles: A Positive Modulator of Innate Immune Responses in Plants. *Sci. Rep.* **2015**, *5* (1), No. 15195.
- (12) Goswami, P.; Mathur, J.; Srivastava, N. Silica Nanoparticles as Novel Sustainable Approach for Plant Growth and Crop Protection. *Heliyon* **2022**, *8* (7), No. e09908.
- (13) Thomas, B.; Raj, M. C.; B, A. K.; H, R. M.; Joy, J.; Moores, A.; Drisko, G. L.; Sanchez, C. Nanocellulose, a Versatile Green Platform: From Biosources to Materials and Their Applications. *Chem. Rev.* **2018**, *118* (24), 11575–11625.
- (14) Alhamid, J. O.; Mo, C.; Zhang, X.; Wang, P.; Whiting, M. D.; Zhang, Q. Cellulose Nanocrystals Reduce Cold Damage to Reproductive Buds in Fruit Crops. *Biosyst. Eng.* **2018**, *172*, 124–133.
- (15) Ning, L.; You, C.; Jia, Y.; Chen, J.; Zhang, Y.; Li, X.; Rojas, O. J.; Wang, F. Cellulose Nanocrystals for Crop Protection: Leaf Adhesion and Controlled Delivery of Bioactive Molecules. *Green Chem.* **2023**, 25 (7), 2690–2698.
- (16) He, Q.; Wang, Q.; Zhou, H.; Ren, D.; He, Y.; Cong, H.; Wu, L. Highly Crystalline Cellulose from Brown Seaweed Saccharina Japonica: Isolation, Characterization and Microcrystallization. *Cellulose* **2018**, 25 (10), 5523–5533.
- (17) Trilokesh, C.; Uppuluri, K. B. Isolation and Characterization of Cellulose Nanocrystals from Jackfruit Peel. *Sci. Rep.* **2019**, *9* (1), No. 16709.
- (18) Du, L.; Arnholt, K.; Ripp, S.; Sayler, G.; Wang, S.; Liang, C.; Wang, J.; Zhuang, J. Biological Toxicity of Cellulose Nanocrystals (CNCs) against the luxCDABE-Based Bioluminescent Bioreporter *Escherichia Coli* 652T7. *Ecotoxicology* **2015**, 24 (10), 2049–2053.
- (19) Kokol, V.; Novak, S.; Kononenko, V.; Kos, M.; Vivod, V.; Gunde-Cimerman, N.; Drobne, D. Antibacterial and Degradation Properties of Dialdehyded and Aminohexamethylated Nanocelluloses. *Carbohydr. Polym.* **2023**, *311*, No. 120603.
- (20) Souza, C. D. A.; Li, S.; Lin, A. Z.; Boutrot, F.; Grossmann, G.; Zipfel, C.; Somerville, S. C. Cellulose-Derived Oligomers Act as Damage-Associated Molecular Patterns and Trigger Defense-Like Responses. *Plant Physiol.* **2017**, *173* (4), 2383–2398.
- (21) Denoux, C.; Galletti, R.; Mammarella, N.; Gopalan, S.; Werck, D.; De Lorenzo, G.; Ferrari, S.; Ausubel, F. M.; Dewdney, J. Activation of Defense Response Pathways by OGs and Flg22 Elicitors in Arabidopsis Seedlings. *Mol. Plant* **2008**, *1* (3), 423–445.
- (22) Luna, E.; Pastor, V.; Robert, J.; Flors, V.; Mauch-Mani, B.; Ton, J. Callose Deposition: A Multifaceted Plant Defense Response. *Mol. Plant-Microbe Interact.* **2011**, 24 (2), 183–193, DOI: 10.1094/MPMI-07-10-0149.
- (23) Savary, S.; Willocquet, L.; Pethybridge, S. J.; Esker, P.; McRoberts, N.; Nelson, A. The Global Burden of Pathogens and Pests on Major Food Crops. *Nat. Ecol. Evol.* **2019**, 3 (3), 430–439.
- (24) Miller, S. A.; Ferreira, J. P.; LeJeune, J. T. Antimicrobial Use and Resistance in Plant Agriculture: A One Health Perspective. *Agriculture* **2022**, *12* (2), 289.
- (25) Ross, A.; Somssich, I. E. A DNA-Based Real-Time PCR Assay for Robust Growth Quantification of the Bacterial Pathogen Pseudomonas Syringae on Arabidopsis Thaliana. Plant Methods 2016, 12 (1), 48.
- (26) Bisceglia, N.; Gravino, M.; Savatin, D. V. Luminol-Based Assay for Detection of Immunity Elicitor-Induced Hydrogen Peroxide Production in *Arabidopsis Thaliana* Leaves. *Bio-Protocol* **2015**, *S* (24), No. e1685, DOI: 10.21769/BioProtoc.1685.